17th World Conference on Earthquake Engineering, 17WCEE
Sendai, Japan - September 13th to 18th 2020

DISTRIBUTED OPTICAL FIBER FOR LABORATORY AND FIELD TESTING IN CONCRETE STRUCTRES

G. Rodriguez(1), J. R.Casas(2), A. Barrias(3) and S. Villalba(4)

(1) *Assistant Professor, Institute of Engineering, National Autonomous University of Mexico UNAM, grog@pumas.ii.unam.mx*
(2) *Professor, Technical University of Catalonia, UPC-Barcelona Tech, joan.ramon.casas@upc.edu*
(3) *PhD researcher, Technical University of Catalonia, UPC-Barcelona Tech, antonio.de.sousa.barrias@gmail.com*
(4) *Assistant Professor, Technical University of Catalonia, UPC-Barcelona Tech, sergio.villalba@upc.edu*

Abstract
This paper outlines the principal results of laboratory and field testing in concrete structures to show the capabilities of distributed optical fiber sensors (DOFS) in their application to monitoring concrete structures. In the first part of this paper, a methodology to obtain the mean shear crack width in concrete beams is proposed. This methodology is based on the laboratory experimental data obtained by a DOFS bonded to the surface of two pre-stressed partial concrete (PPC) beams subjected to shear test with increasing levels of load. The results show the feasibility of the proposed method in calculating the shear crack width when compared to the results from traditional instrumentation. In the second part of the paper, a monitoring process by DOFS on a real world structure is described. The principal results of the enlargement of a pre-stressed concrete bridge are presented. The versatility and easy installation of DOFS compared with traditional monitoring systems is an important characteristic to consider in its application when monitoring real world structures. The DOFS used in this study provide continuous (in space) strain data along the optical fiber with high spatial resolution in the order of millimeters. This study verifies that the OBR technique is applicable in real conditions and confirms the high accuracy inherent to the optical fiber technology. The use of the OBR technique is not only able to detect appearing cracks, but also to perform a global structural behavior monitoring. For this reason, this technique is an important alternative to cover the limitations (number of points interrogated) of the discrete sensors such as strain gauges or LVDT´s, with which only local data is obtained.

Keywords: distributed optical fiber sensors, monitoring system, concrete structures, crack detection

1. Introduction
Around the world, civil engineering infrastructure is subjected to several events that deteriorate and compromise their structural integrity throughout their service lifetime. Implementing of damage identification strategies for infrastructure it has been one of the most studied and researched fields in the past three decades within the engineering and academic communities due to its vital importance and potential to allow better decision making by infrastructure owners and agencies. The use of sensor-based monitoring systems improves structural health monitoring strategies by improving their efficiency and accuracy, here the optical fiber sensors have gained an important place and their use is increasingly being accepted. Their small dimensions, rapid data transmission and immunity from electromagnetic influences are some of the advantages of the discrete optical sensors over electrical traditional instruments [1,2]. Even so, discrete sensors can only provide punctual measurements, and important data away of the sensors could be lost. To deal with the above limitation, optical fiber ability of monitoring physical fields (strains and temperatures) has been exploited to develop different distributed optical fiber sensor systems (DOFSs). DOFS share the same advantages of discrete optical fiber sensors, however they offer the unique ability of monitoring strain and temperature variations with spatial continuity along the optical fiber. In this paper the Optical Backscatter Reflectometry (OBR) is applied to obtain strain and temperature measurements with high spatial resolution [3].

2. Measurement technique

A DOFS is usually applied by measuring physical changes along the length of a sensing fiber optic. This is a distinctive property of DOFS with respect to other measuring techniques, because it can replace a several number of discrete sensors. DOFSs are generally based on the measuring of some perturbations induced on the light that travels inside the fiber. In this article OBR has been applied to the measurement of strain and temperature with a spatial resolution around millimeters. Basically, the OBR system part is a monitoring unit that throws a beam of light, usually a laser of adjustable frequency, to which an optical fiber cable is connected. The characteristics of the beam of light traveling within the fiber are known, and they change depending on the temperature and the strain at which the fiber is subjected. This process is shown in Fig. 1. More information on this measurement technique is available in previous studies [4,5].

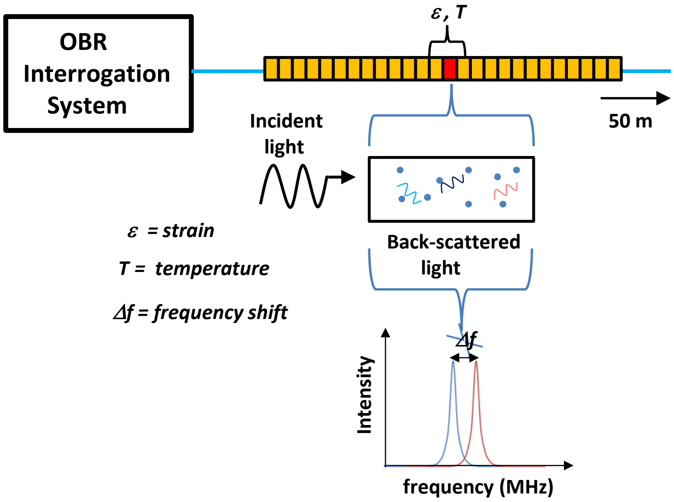

Fig. 1. Rayleigh scattering measurement process.

3. Proposed Methodology to obtain the shear crack pattern

Based on the case of crack pattern identification of concrete elements in bending [4, 5], the proposed method for the shear case is based on the analysis of the strain profile along a DOFS. However, due to the unknown inclination of the shear cracks, to detect and locate the crack and obtain the crack width, a monitoring method must be established to determine the strain distribution in at least two perpendicular directions. Thus, an arrangement with one DOFS is proposed to form a grid within the area in which these cracks are expected to occur (zone of maximum shear within the element). A schematic representation of this mesh is shown in Fig. 2. A peak in the strain profile measured by the fiber will appear in the location where a crack will form. This will be used to detect and locate the crack. The strain profiles in two orthogonal directions will serve to obtain the inclination of the crack and derive the crack width.

From here, when load is applied, strain profile in two perpendicular directions is obtained at the zone of interest. Through the coordinates (x_n, y_n), any measuring DOFS point is identified. These coordinates are a function of the spatial resolution assigned in the OBR system, which in this case was of 1 cm. In the case of the 2D mesh, the spatial resolution is translated into the increment Δx and Δy between the coordinates x_n, y_n in both directions, as indicated in Fig. 2. Afterwards and through the analysis of the information obtained with the OBR system, the tracing of progressive cracking pattern in the instrumented area can be achieved.

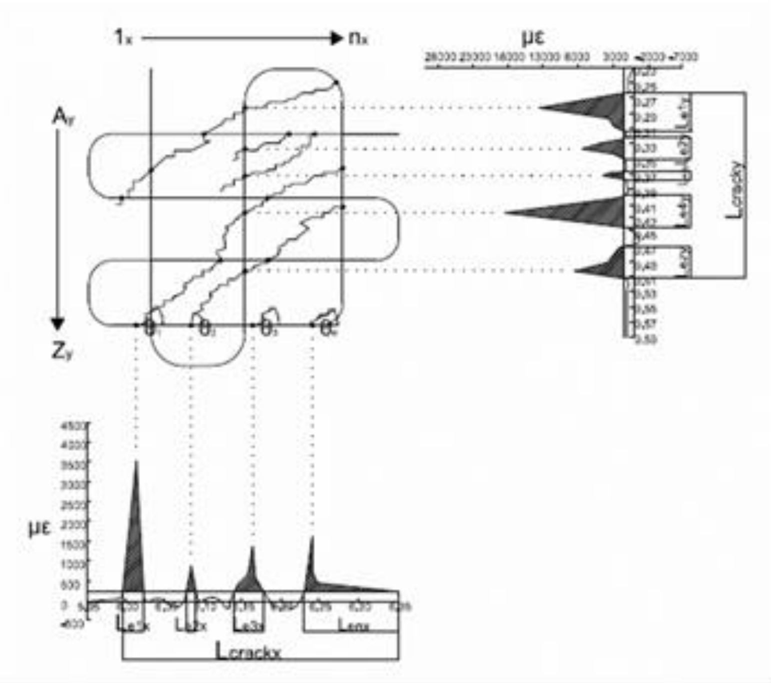

Fig. 2. Procedure for locating, tracing and calculating shear crack widths.

The strain variation along the fiber allows to identify the moment when cracking starts and its evolution through the loading process. A complete description of the methodology is available in [6,7]. In the 2D mesh formed by the DOFS, one or more cracks are detected simultaneously in two orthogonal directions X and Y for a given value of the test load. In this way, Eq. 1 can be established for the DOFS in direction X. The right side of Equation 1 represents the mean strain in the cracked zone in direction X as the integral of the strain in each of the n effective lengths (L_{eix}) where a crack is present.

$$\varepsilon_{\text{mean x}} = \frac{1}{L_{e\ total\ x}} \sum_{i=1}^{n} \int_0^{Leix} \varepsilon_{\text{OBRix}}\, dx \qquad (1)$$

Where:

$$L_{e\ total\ x} = \sum_{i=1}^{n} L_{eix}$$

A similar process is carried out with the vertical strain data.

On other hand, the mean strain (ε_{mean}) in both X and Y directions, can also be obtained from Eq. 3 and 4.

$$\varepsilon_{meanx} = \varepsilon_{fctx} + \frac{\sum wx}{L_{crackx}} \qquad (3)$$

$$\varepsilon_{meany} = \varepsilon_{fcty} + \frac{\sum wy}{L_{cracky}} \qquad (4)$$

Then, equating Eq. (1) with equations (3) and (4), the value of the summation $\sum w$ can be obtained

$$\frac{1}{L_{e\,total\,x}}\sum_{i=1}^{n}\int_{0}^{Lei\,x} \varepsilon_{OBRi\,x}\,dx = \varepsilon_{fctx} + \frac{\sum wx}{L_{crack\,x}} \qquad (5)$$

$$\frac{1}{L_{e\,total\,y}}\sum_{i=1}^{n}\int_{0}^{Lei\,y} \varepsilon_{OBRi\,y}\,dy = \varepsilon_{fcty} + \frac{\sum wy}{L_{crack\,y}} \qquad (6)$$

In equations 5and 6, $\sum wx\ and\ \sum wy$ comprises the sum of the widths of all cracks w_x or w_y that occur within the cracked length. In this way, an average crack width is obtained in each direction x, y:

$$w_{mean\,x\,or\,y} = \frac{\sum w_{\ x\,or\,y}}{n} \qquad (7)$$

In equation 7 n is the number of cracks and is obtained by counting the peaks that occur in the continuous strain profiles of the OBR experimental results.
Finally, the average crack width is obtained through Ec. (8):

$$w_{mean} = \sqrt{w_{mean\,x}^{2} + w_{mean\,y}^{2}} \qquad (8)$$

4. Experimental validation

To evaluate and verify the method proposed in the previous section to monitor the crack width in concrete elements subject to shear, two partially pre-stressed concrete (PPC) beams with 8 m span-length denominated I-2 and I-3 were tested. A three-point load test with the point load applied at a distance of 2 m from one of the supports of each beam were carried out as shown schematically in Fig. 3. The test is designed to produce the shear failure of the beam.

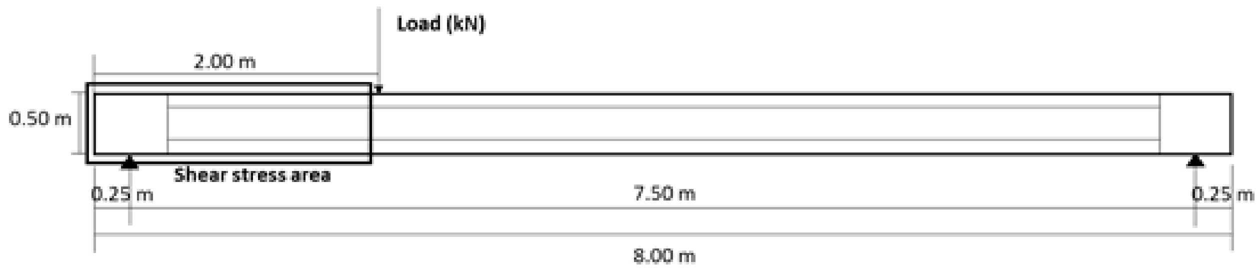

Fig. 3. Shear test set up of beam I-2 and I-3.

To measure and compare experimentally the different crack widths, DOFS 2D mesh and displacements rosettes as shown in Figs. 4 and 5 were placed in the web of each beam. In the two tested beams the displacements rossettes are conformed by two quadrilateral arrangements with 25 cm of length as shown in Figs. 6 and 7. The DOFS 2D grids were conformed in the web of the two tested beam with one DOFS of 10 m in length. Also in these figures, the dimensions of the transversal section of each beam are shown. The only difference between two tested beams was the web thickness, 120 and 180 mm for beam I-2 and I-3 respectively. The horizontal grid sections were nominated with capital letters and the vertical sections were labeled using the numbers 1 to 10 (Figs. 4 and 5).

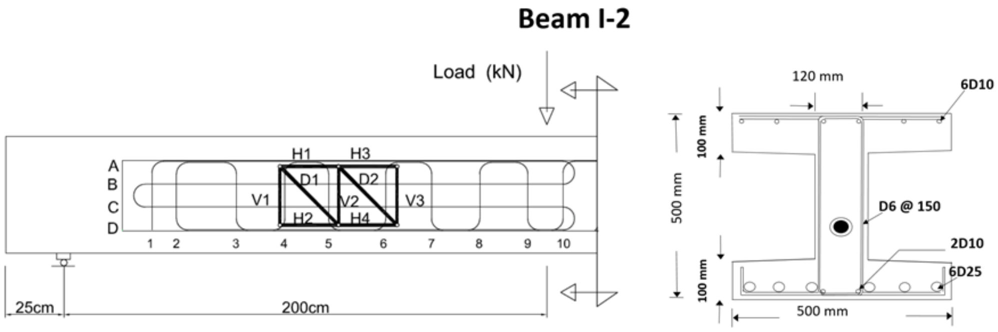

Fig. 4. DOFS and displacement rosette to shear test of beam I-2.

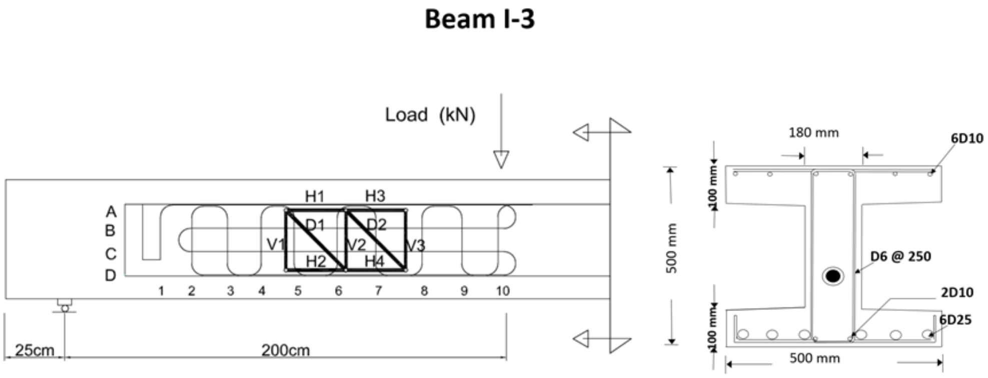

Fig. 5. DOFS and displacement rosette to shear test of beam I-3.

Also from Figs. 4 and 5 each of the potentiometers that conform the displacement rosettes are identified. V1, V2 and V3 are vertical potentiometers, the upper horizontals H1 and H3, the lower horizontals H2 and H4, and the diagonals D1 and D2. The separation between the vertical potentiometers was approximately 25 cm, which involved covering a region of the web beams of approximately 50 cm (Figs. 4 and 5). The mechanical properties of the concrete are presented in Table 1, where f_{cm} is the mean concrete compressive strength, f_{ct} is the concrete tensile strength and E is the concrete elasticity modulus. The values of ε_{fct} are the maximum tensile concrete strain. All these values were obtained by the testing of the specimens moulded during the pouring of the beams and tested after 28 days.

Table 1. Concrete mechanical properties

Beam	f_{cm} (Mpa)	f_{ct} (Mpa)	E (Mpa)	ε_{fct} $\mu\varepsilon$
I-2	29.4	4.15	27264	152
I-3	41.5	5.86	34261	171

Based on the previous experiences by the authors in deploying DOFS in concrete structures, and a basic guidance on the bonding of these sensors established by the supplier [15] a bonding DOFS protocol was followed. This protocol is described in detail in [6,7]. The DOFS used was a single-mode fiber with a coating of a polymer (polyimide) to protect the fiber against scratches and environmental attack. Firstly, bond areas were cleaned and free from grease. A commercial glue was applied to the bond area (on the delimited shear zone of the web of each tested beam), avoiding to apply adhesive in excess. The glue used was an epoxy because some experiences [8] have shown that in the laboratory environment, the installation with epoxy produces better results than using cyanoacrylate adhesives in concrete surfaces. According to that, a commercial bicomponent epoxy adhesive (Araldit) was applied to the bond area. The adhesive was applied to one of the bond surfaces, avoiding the use of tissue or a brush to spread the adhesive.

The two beams I-2 and I-3 were tested under quasi-static load, applied gradually and with six loading and unloading cycles. The applied force was controlled by displacement of 1 and 2 mm / min, until the beams failed. The loading sequence is shown in Fig. 6. In this figure the total history of loading is indicated with a dash line. The DOFS break point is shown with a point and a continuous line. It is important to notice that from a certain level of load (indicated with a point and a thick continuous line). Detection and location of shear cracks is limited to load levels around 260 and 258 kN for the beams I-2 and I-3 respectively. In any case, these load levels produce high cracking and large deflections and therefore are far beyond the normal service load levels expected in real structures. A view of the experimental test setup is shown in Fig. 7. A complete and detailed description of the test results is available in [6,7].

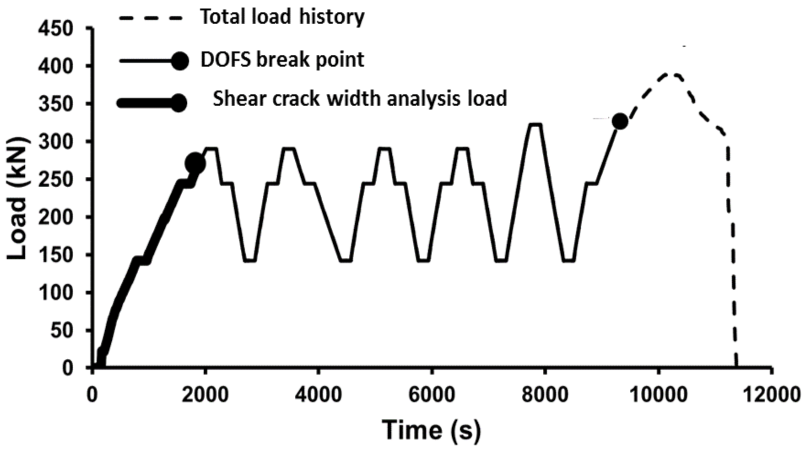

Fig. 6. Total loading sequence and part monitored with the DOFS 2D mesh in the tests

Fig. 7 Global view of experimental test of beams.

5. Results of PPC beams laboratory test

Using a coordinate system (x_n, y_n), as previously described, the location of appearing cracks was obtained. Thanks to 1 cm OBR system spatial resolution, the strain variation in the DOFS mesh of the tested beams could be obtained. In this way, both strain profiles in horizontal and vertical directions were measured simultaneously. In the right side of Fig. 8, one example of the horizontal strain evolution in the I-3 tested beam versus different load levels from 198 to 258 kN is shown. During the tests and to establish the order of appearance of the cracks, the sampling rate of the OBR system was 5s along the DOFS length. Once the crack points have been detected and located, it is also possible to obtain the strain values in the web for increasing load levels. Additional information is available in [6,7].

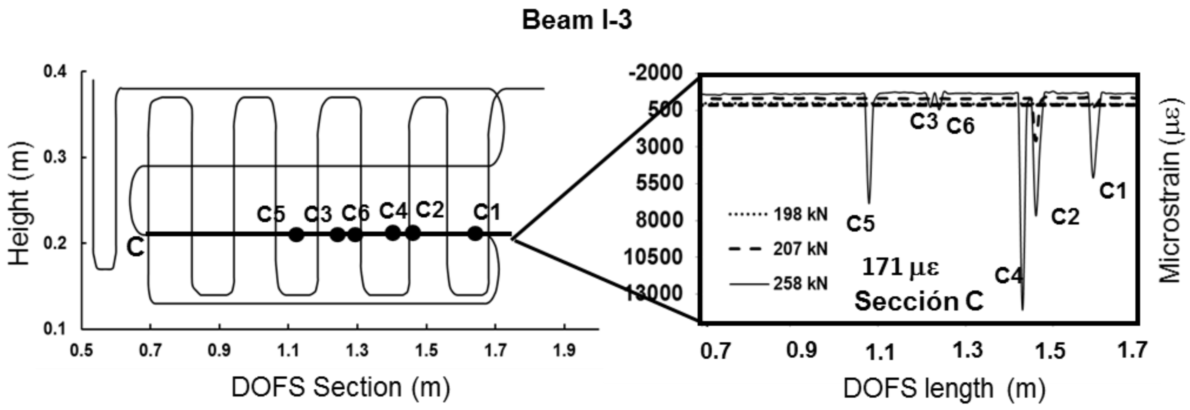

Fig. 8. Strain distribution and crack location in horizontal section C of beam I-3 at different load levels.

Through the analysis of the information obtained with the OBR system, the tracing of different cracking patterns in the 2D DOFS mesh area was achieved progressively as load was increasing. The shear crack patterns in the beams obtained with the DOFS strain data were validated thanks to the visual inspection carried out and photos taken during the test execution. In Fig. 9 one example of this validation is shown. Calculation of the average crack width was limited to the load level shown in Fig. 6. Therefore, continuous strain data were used to obtain the average crack width in each tested based on the methodology described in the section 3 of the paper. Examples of the average shear crack widths obtained with the OBR method and the displacement values from the rosette placed in the web of beam I-2, are shown for comparison in Table 2. The diagonal potentiometers D1 and D2 shown in Fig. 4 were considered for comparison. Additional comparisons are available in [6,7]. In general, the order of magnitude of the crack widths obtained in each type of instrumentation is similar, especially for the load levels in which the crack widths begin to be significant. It should be taken into account that the comparison of results can only be done in an averaged way within the total cracked zone covered by the rosette´s displacements.

6. Urban bridge monitoring

This bridge is located at one of the main entrances of the city of Barcelona, Spain. It is a simply-supported two span bridge with span-lengths of 36 and 50 m (Fig. 10). Each span consists of three box-girder prestressed concrete beams connected by an upper reinforced concrete slab (Fig. 11). This structure allows the crossing of vehicles and pedestrians in both directions through the use of two road lanes and sidewalks. As a result of the change in the load pattern of the bridge, it was decided to carry out the monitoring of the enlargement process in order to detect major changes in the structural behaviour of the bridge and obtain information to assess the structural safety during and at the end of the construction work using DOF sensors since this technology does not require a reference to the ground.

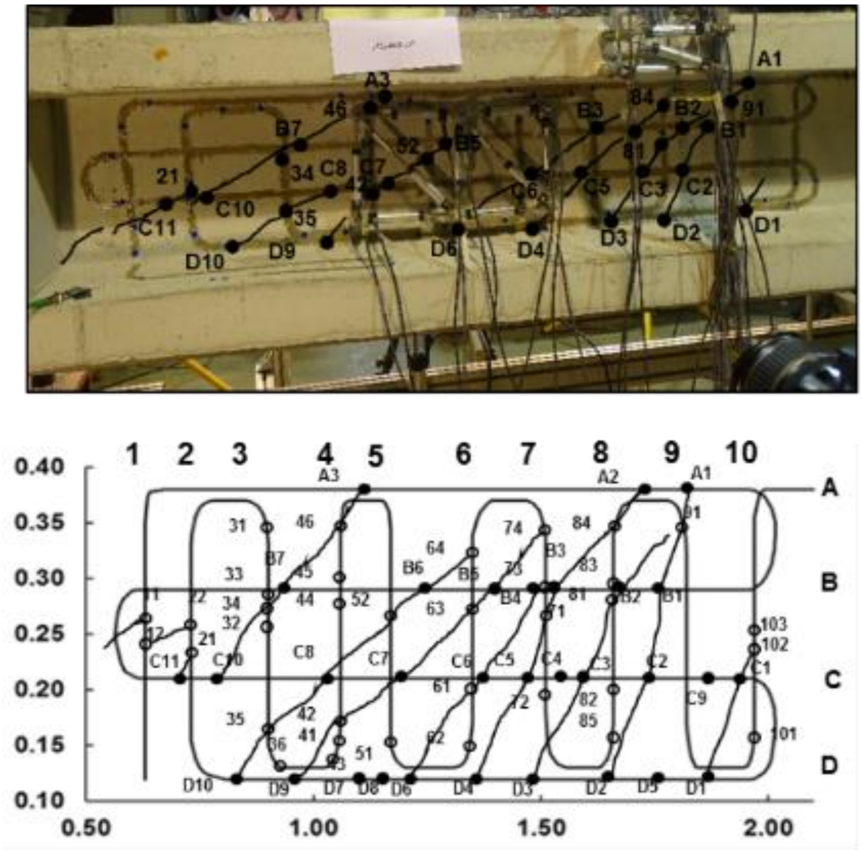

Fig. 9. Real cracking pattern and obtained with DFOS in beam I-2 at a load of 203 kN.

Table 2. Comparison of average crack widths D1, D2 and wOBRt for beam I-2

Load (kN)	D1_ponten (mm)	D2_ponten (mm)	*wOBRx* (mm)	*wOBRy* (mm)	*wOBRt* (mm)
100	0.023	0.000	0.060		0.060
142	0.038	0.048	0.079	0.065	0.102
260	0.337	0.345	0.185	0.179	0.258

The DOFS were placed inside the box girder allowing for an expected better protection of the sensors and an easier access for their installation and operation (Fig. 11). Due to the anticipated long duration of the monitoring period in this application, the correct and careful implementation of these sensors assumes an even greater importance since any potential rupture or misuse of the fiber may compromise its performance. In this way, the use of two sensors instead of one also provides a desirable redundancy that allows a lower probability of loss of monitoring data (Fig. 11).

7. Results of monitoring urban bridge

The results obtained with both 50 m of optical fibers (36 m of which were bonded to the structure, adjusting to the span length) are analysed. Consequently, in this application, OBR was performed in a way that 3600 points were interrogated simultaneously with a spatial resolution of 1 cm. The information acquired by the DOFS corresponds to continuous readings obtained in combined time intervals of: 1 reading each 5 minutes and 1 reading each 10 minutes. From this large amount of data, the critical values (maximum and minimum) are analysed and used to generate envelope response graphs.

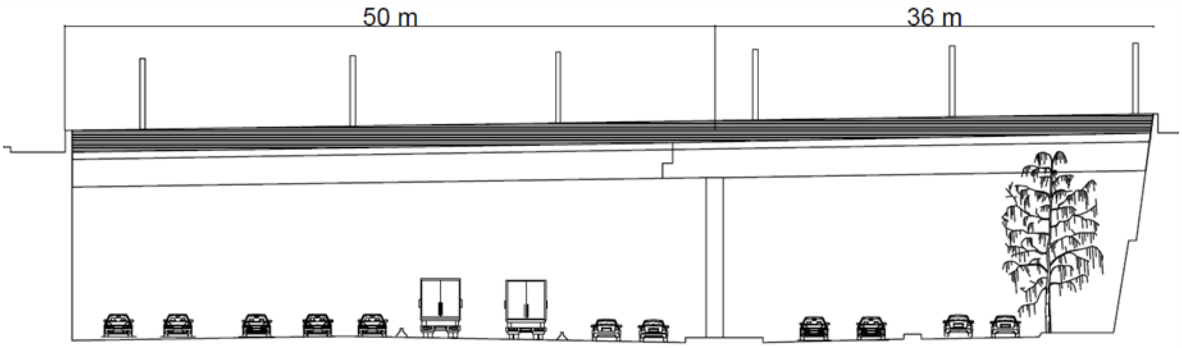

Fig. 10. Urban bridge monitored in Barcelona, Spain

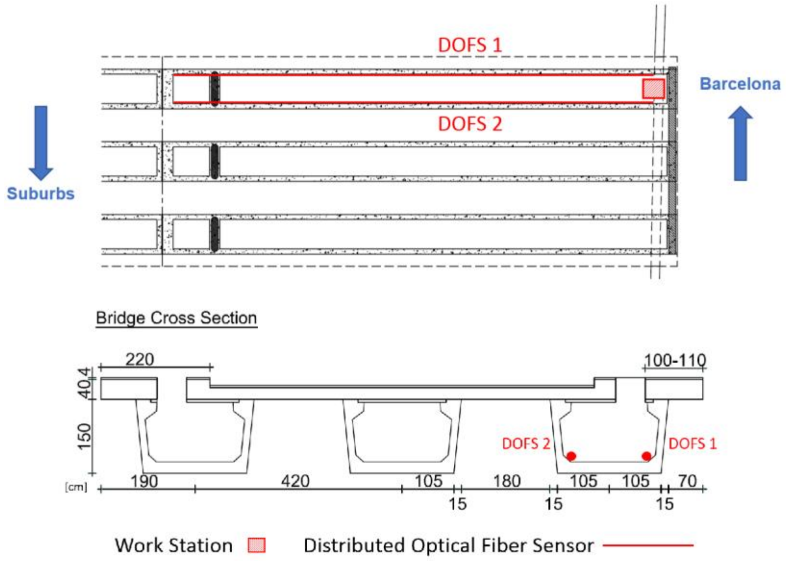

Fig. 11. General scheme of DOFS monitoring

In left side of the Fig. 12, it is possible to observe the evolution of the strains measured by the DOF 2 for the different measured events, comparing the readings of each one with their first reading in a monitoring period that extended through 6 months. It is important to point out, that this comparison is made with measurements from different days taking the care of selecting readings within the similar time interval period in order to mitigate the influence of daily time dependent phenomenon. Regarding the measurements of DOF 2, from the first reading conducted on August to the remaining ones, one may recognize an increment of compression strains. Hence, in this period, it was detected by both deployed fibers the increase of compression strain measurements of the monitored bridge. This was a result of the construction works being done in this time window, such as the removing of asphalt layers and some bridge equipment in the first stages of the procedure and naturally the effect of the temperature variation from Summer to Winter.

Furthermore, due to this relatively long monitoring period, the observed temperature variation not only affects the structure's behaviour but also the readings of the DOF sensors. Both the refractive index of the backscattered light and the materials which compose the sensors are dependent of these temperature changes so a compensation of its effect on the monitoring output is required. In order to take into account these effects, in terms of spectral shift, the thermal output, Δv_T can be expressed as Eq. (9)

$$\Delta v_T = \Delta v_n + \Delta v_S \qquad (9)$$

Where Δv_n represents the refractive index-dependent spectral shift and Δv_S is the coefficient of thermal expansion-dependent spectral shift. For the situation where there aren't significant local temperature gradients throughout the length of the optical fiber, this method can be used for compensation. In this case, a relatively short fiber loop can be created by leaving a small part of the sensor lying down on the monitored structural element without bonding it, as represented in Fig. 13. One way to perform this thermal induced error compensation for measurements performed by OBR based DOFS where the thermal conditions are variable and where non-adhered segments of the DOFS are present, is available in [8].

With this method, in order to obtain the pure mechanical strain generated during the monitoring period, it is necessary to subtract from the strain obtained in the bonded part of the fiber both the effects of the refractive index dependent apparent strain and the coefficient of thermal expansion dependent apparent strain [8]. This was the method adopted in this real-world monitoring application, by the use of the unbonded loop segment of the fiber located at the its end, inside the beam, as seen in the right side of the Fig. 12. From these results, the effect of the general unloading that the bridge suffered due to the removal of the slabs, pavement and the milling of the agglomerate, when compared to the loading values at the time of calibration and the structure's shrinkage behaviour induced by the decrease of temperature, is further evidenced.

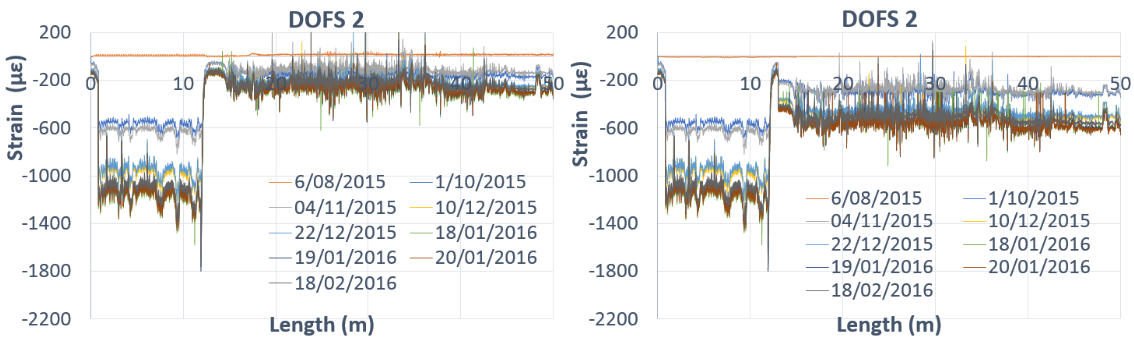

Fig. 12. Comparison of DOFS 2 readings before (left) and after temperature compensation (right).

Furthermore, this continuous increase of compression of the bottom fiber of the monitored span is also explained by a higher induced load on the adjacent span compared to the one applied to the instrumented span. Due to the presence of the large peaks, the strain is possibly masked and its real distribution along the instrumented box-girder is not clear. To observe a better strain distribution, a spatially averaging only of the mechanical strains for S1, S2, S3 and S4 segments was performed and plotted in Fig.14. The values are presented in Table 3. In segment S1, mean mechanical strain values lower than those generally present in the rest of the DOFS length can be shown. This decrease is due to the influence of the support system (elastomeric bearings) on the bridge kinematics.

Fig. 13. Unbonded loop of the DOFS.

The mean mechanical strain distribution is almost uniform in the rest of the box-girder as shown the values of Table 3. This means that the applied forces in the deck that could produce variations of strain along the bottom part of the bridge were very small at the time of measuring the sensors, being therefore the strain mainly due to the uniform shortage of the box-girder associated to the decrease of temperature from summer to winter. Note that the difference in strain between August and February in the order of 500 microstrain (Fig.) is very much plausible for a bridge like this and the climate in Barcelona.

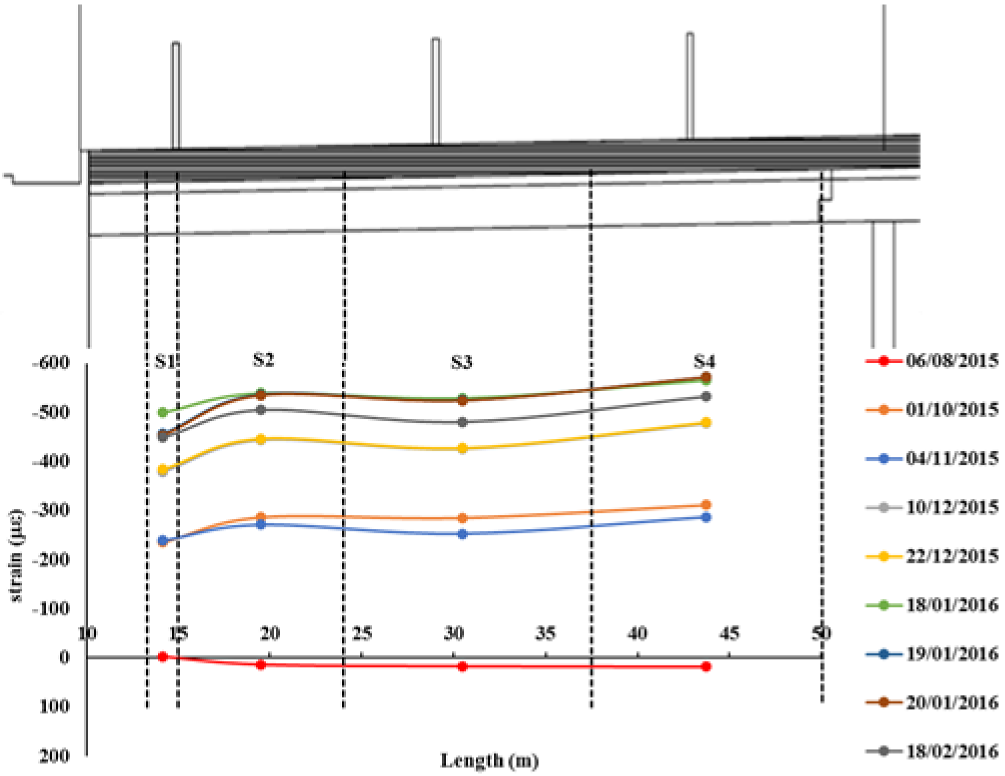

Fig. 14. Mean mechanical distribution for DOFS2 from summer to winter

Table 3. Section localized temperature compensation for DOFS2.

Segment ID	2015-1	2015-2	2015-3	2015-4	2015-5	2016-1	2016-2	2016-3	2016-4
S0	14.1	-707.7	-771	-1168.5	-1177.5	-1393.4	-1383.2	-1397.4	-1353.6
S1	5.5	-235	-238.7	-379.1	-383.6	-499.5	-456.2	-453.5	-448.8
S2	17.1	-286	-271.2	-443.8	-446.2	-539	-536.5	-534.8	-504.8
S3	19.8	-284.9	-253	-425.6	-426.9	-528.7	-524.4	-524.1	-480.4
S4	20.7	-311.1	-287	-477.4	-479.3	-565.2	-571.7	-571.6	-532.3

8. Conclusions

In this paper, the successful application of DOFS, on experimental tests and the structural health monitoring of a real structure were presented. In the first instance the potential application of DOFS in the monitoring of shear cracking in concrete structures was the main purpose of the experimental tests described. A methodology is presented, not only to detect cracking, but also to locate the cracks and thus, allowing to conform the corresponding cracking patterns in the element due to the shear effect. It is also possible to monitor the evolution of the cracking pattern for different levels of load. The method has been checked in a series of laboratory tests carried out in partially pre-stressed concrete beams. Therefore, the proposed method can be seen as a feasible technique for the SHM of concrete elements subjected to shear actions. In relation to application of DOFS on the monitoring of an urban bridge, it was possible to follow and monitor the structural behaviour in this structure during the different procedures executed with the use of a relative small number of sensors and simple monitoring systems. With the DOFS readings at different dates, it was possible to easily detect the stresses increments in the structure and in this way, assess their structural safety. If anomalous changes were detected with the instrumentation, automatically the works would stop and necessary corrective measures would be taken. Furthermore, the evolution of strain variation along an extensive length of structure was achieved with a relatively simple and easy installation of only one sensor and one connection to a reading terminal. In conclusion, all of this serving as practical evidence for designers and rehabilitation engineers of the potential, advantages and disadvantages of the use of this sensing technology. Nevertheless, with the results obtained in this work, the OBR theory associated with DOFS proved its reliability in SHM of civil engineering applications and continues to showcase the promising future of monitoring systems based on this technology.

9. References

[1] Casas J, Cruz P (2003): Fiber optic sensors for bridge monitoring. *Journal of Bridge Engineering*, **8** (6), 362-373.

[2] Glisic B, Inaudi D (2012): Development of method for in-service crack detection based on distributed optical fiber sensors. *Structural Health monitoring*, **11** (2), 161-171.

[3] Güemes A, Fernández-López A, Soller B (2010): Optical fiber distributed sensing-physical principles and applications. *Structural Health monitoring*, **9** (3), 233-245.

[4] Casas J, Villalba S (2014): Management and safety of existing concrete structures via optical fiber distributed sensing. *Chapter of the book Maintenance and Safety of Aging Infrastructure*, CRC Taylor and Francis.

[5] Rodríguez G, Casas J, Villalba S (2015): Cracking assessment in concrete structures by distributed optical fiber. *Structural Health monitoring*, **24**, 035005 11pp.

[6] Rodríguez G, Casas J, Villalba S (2019): Shear crack width assessment in concrete structures by 2D distributed optical fiber. *Engineering Structures*, **195**, 508-523.

[7] Rodríguez G, Casas J, Villalba S (2019): Shear crack pattern identification in concrete elements via distributed optical fiber grid. *Structure and Infrastructure engineering*, doi.org/10.1080/15732479.2019.1640256.

[8] Barrias A, Rodríguez G, Casas J, Villalba S (2018): Application of distributed optical fiber sensors for the health monitoring of two real structures in Barcelona. doi.org/10.1080/15732479.2018.1438479.

